Cell Reports, Volume *31*

Supplemental Information

Functional Divergence of the *Arabidopsis* Florigen-Interacting bZIP Transcription Factors FD and FDP

Maida Romera-Branchat, Edouard Severing, Chloé Pocard, Hyonhwa Ohr, Coral Vincent, Guillaume Née, Rafael Martinez-Gallegos, Seonghoe Jang, Fernando Andrés Lalaguna, Pedro Madrigal, and George Coupland

Supplemental information titles and legends:

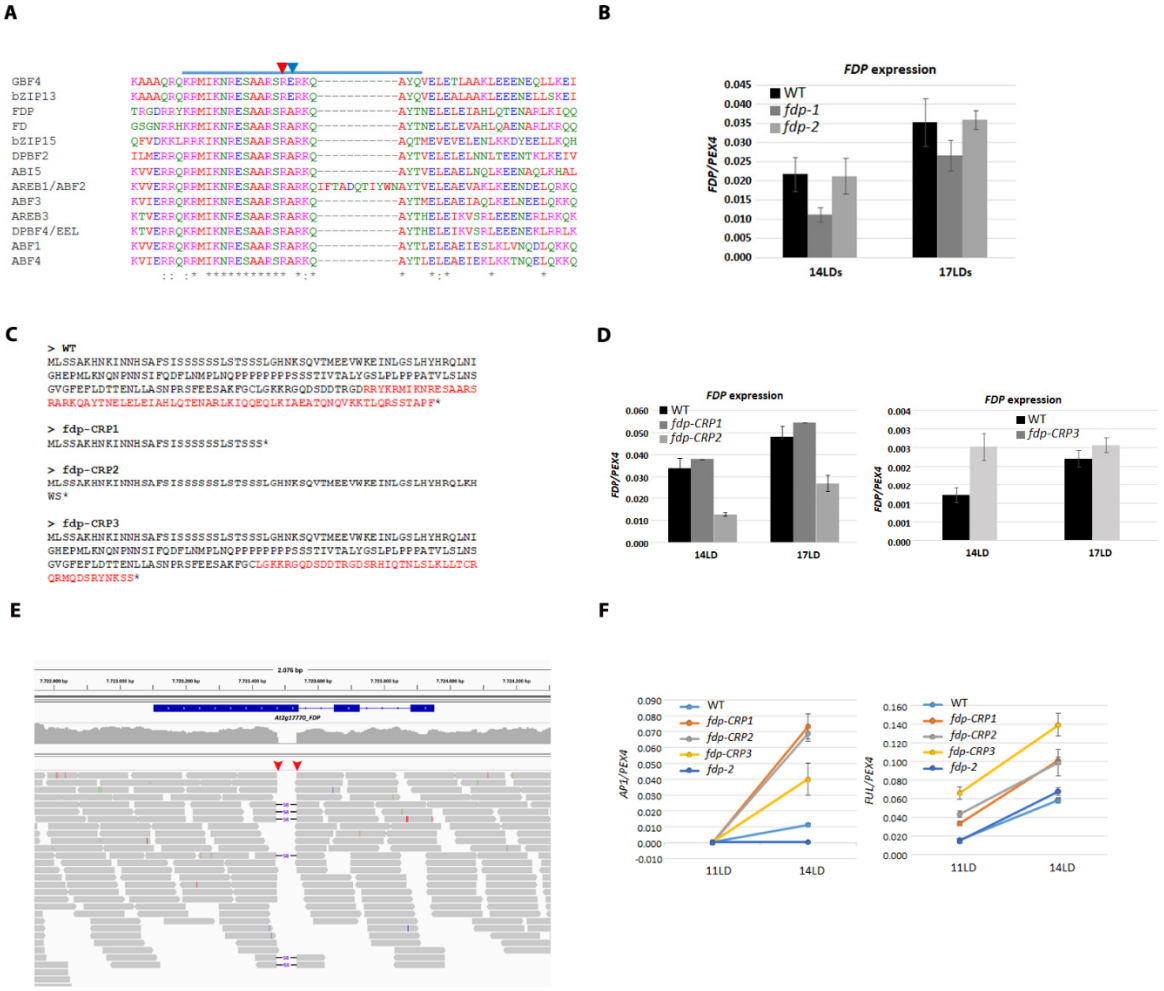

Figure S1. Related to Figure 1. Characterization of *fdp* mutants (TILLING and CRISPR_Cas9 mutants)

(A) ClustalW protein sequence alignment of the bZIP domain of the Arabidopsis Group A bZIP transcription factors. Red and blue arrows mark the predicted amino-acid changes in *fdp-1* and *fdp-2* alleles, respectively. The upper blue line marks the basic region of the bZIP domain. (B) RT-qPCR analysis of *FDP* mRNA levels in WT, *fdp-1* and *fdp-2* apices of 14- and 17-day-old plants. (C) Predicted protein sequences of FDP wild-type (WT) protein (234 amino acids), CRP1-fdp (30 amino acids), CRP2-fdp (62 amino acids) and CRP3-fdp (192 amino acids). All sequences were generated using the Expasy Tool. In the WT sequence, the bZIP domain is highlighted in red; in fdp-CRP1 and fdp-CRP2, frame-shifts in the FDP sequence generate truncated proteins. In fdp-CRP3, a larger deletion of 58 nt in the FDP coding sequence generates a frame-shift that strongly impairs the bZIP domain. (D) RT-qPCR analysis of *FDP* mRNA levels in WT, *fdp-CRP1* and *fdp-CRP2* apices (left graph) of 14- and 17-day-old plants and WT and *fdp-CRP3* apices of 14 and 17-day-old plants (right graph). (E) Whole-genome sequencing reads from the *CRP3-fdp* mutant mapped to the *A. thaliana FDP* locus. The predicted 58-nt deletion in the mutant is confirmed by mapped read alignments containing an indel of the correct size at the predicted position in the genome (red rectangles). (F) RT-qPCR analysis of *AP1* mRNA levels (left graph) and of *FUL*

mRNA (right graph) in WT (Col-0), *fdp-CRPs* and *fdp-2* apices in 11- and 14-day-old plants. One representative biological replicate (out of two) is shown.

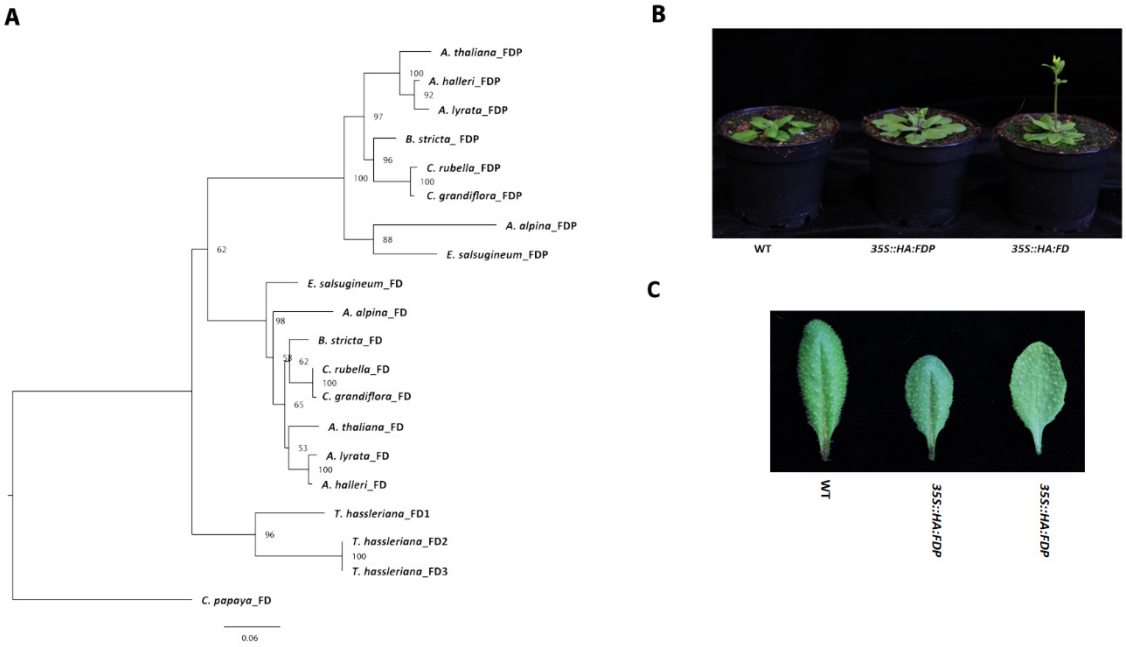

Figure S2. Related to Figure 2. Maximum likelihood tree of FD and FDP sequences.

(A) The tree was constructed using the HKY+G substitution model as recommended by the ModelTest program (see Methods). Branch lengths correspond to the number of expected mutations per site. Bootstrap support (out of 100) is shown at the internal nodes. Eight different Brassicaceae species, including Arabidopsis were used for the analysis (Methods). As an outgroup, *Tarenaya hassleriana* was used. (B) Plants of the illustrated genotypes grown under LDs for 26 days. (C) The sixth rosette leaf of the shown plants harvested from 21-day-old-plants.

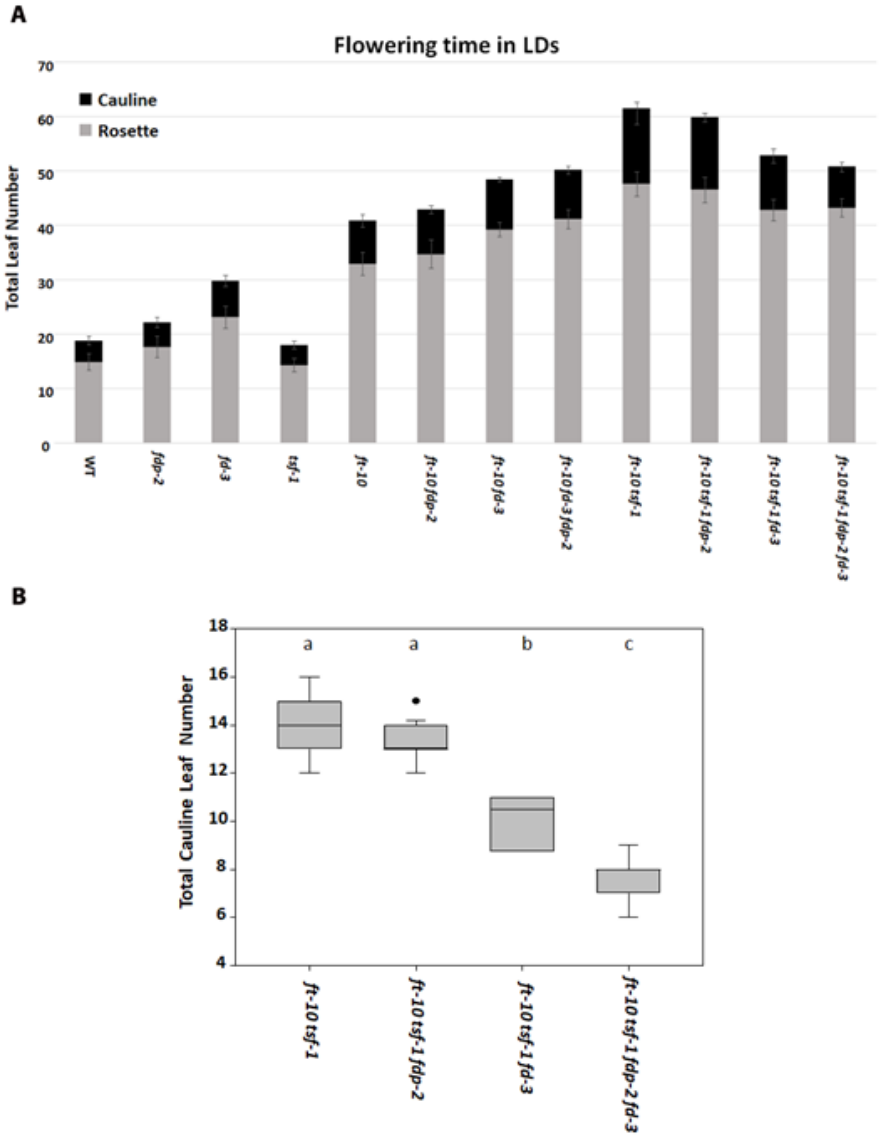

Figure S3. Related to Figure 3. Interaction between FD/FD/FT/TSF in the control of flowering under LDs. (A) Flowering time of WT, *fdp-2, ft-10, fdp-2 ft-10, fd-3 ft-10, ft-10 fd-3 fdp-2, ft-10 tsf-1, ft-10 tsf-1 fdp-2, ft-10 tsf-1 fd-3* and *ft-10 tsf-1 fd-3 fdp-2* grown in LD. (B) Total cauline leaf number of the double mutant *ft-10 tsf-1* compared to the triple and quadruple mutants *ft-10 tsf-1 fd-2, ft-10 tsf-1 fd-3* and *ft-10 tsf-1 fdp-2 fd-3*. Letters shared between genotypes indicate no significant difference in flowering time. One-way ANOVA followed by Dunn's method was used for the statistical analysis. In (B) groups were considered statistically different when $p \leq 0.001$

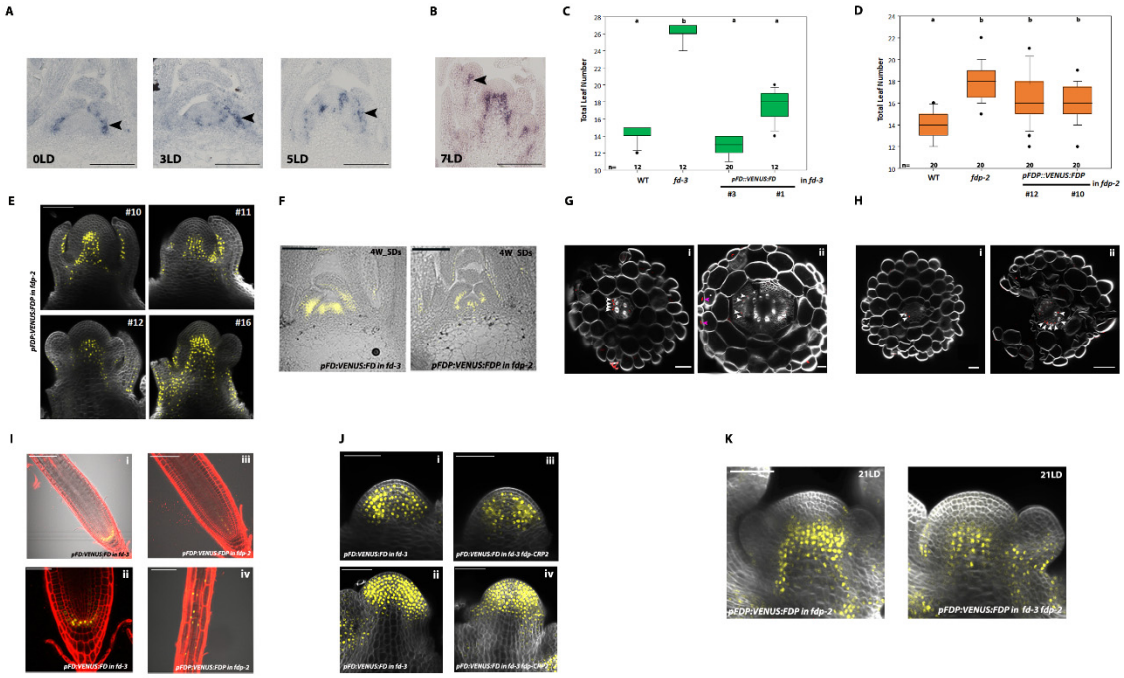

Figure S4. Related to Figure 4. Characterization of *pFD::VENUS:FDP* and *pFDP::VENUS:FDP* transgenic lines. (A, B) *In situ* hybridizations of *FDP* mRNA on apices of plants grown for 3 weeks under SD (0 LD) and then transferred to LDs for 3, 5 days (A) and 7 days (B). Black arrows in A: Adaxial side of leaf. Black arrow in B: center of a young floral bud. (C) Complementation of the *fd-3* flowering phenotype by *pFD::VENUS:FD*. Two representative transgenic lines are shown that fully complement the late flowering phenotype of *fd-3*. (D) Complementation of the flowering time defects of *fdp-2* by *pFDP::VENUS:FDP*. Two representative lines are shown. In this case, *fdp-2* flowering defects are not complemented. (E) Confocal microscopy images of four independent homozygous *pFDP::VENUS:FDP* lines grown for 14 days in LDs. The VENUS:FDP expression domain is similar in the different lines. (F) Cryosections showing VENUS:FD (left panel) and VENUS:FDP (right panel) in apices from 4-week-old plants grown in SDs. (G) Cross sections of hypocotyls showing VENUS:FD from 3 and 14-day-old plants (i, ii). (H) Cross sections of hypocotyls showing VENUS:FDP from 5- and 12-day-old plants (i, ii). VENUS signal is shown in red color. Each white arrow indicates VENUS signal in one cell in the vascular tissue. Pink arrow indicates VENUS signal in the epidermis. (I) Confocal images of VENUS:FD in root tips (i, ii); VENUS:FDP in root tips (iii); and VENUS:FDP in the differentiation zone of the root (vi). Roots were stained with propidium iodide to reveal their cellular organization. (J) Confocal images of VENUS:FD in *fd-3* and VENUS:FD in *fd-3 CRP2-fdp* grown in LDs. The upper two panels show VENUS signal in apices of 10-day-old plants. Lower panels show VENUS signal in the shoots of 17-day-old plants. (K) Confocal images of VENUS:FDP in *fdp-2* and VENUS:FDP in *fd-3 fdp-2* grown in LDs. The two panels show VENUS signal in apices of 21-day-old plants. Letters shared between genotypes in (I) and (K) indicate no significant difference in flowering time. One-Way ANOVA followed by Dunn's test was used for the statistical analysis; $p < 0.05$. Scale bar= 50µm (A, B, Gii, Iii, J and K); 100µm (E, F, Ii, Iiii and Iiv); 20µm (Gi, Hi and Hii).

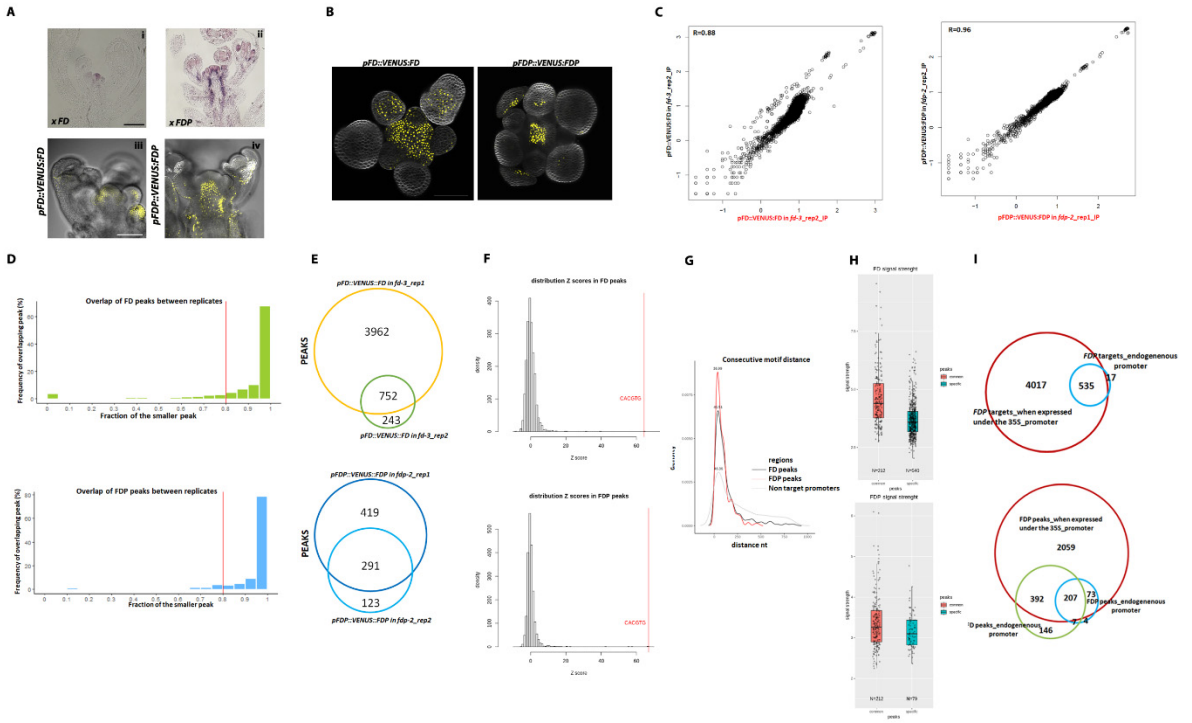

Figure S5. Related to Figure 5. ChIP seqs of FD and FDP. (A) *In situ* hybridization with *FD* (i) and *FDP* (ii) probes on apices of 25-day-old plants. (iii, iv). Confocal images of VENUS:FD and VENUS:FDP protein expression in inflorescence apices of 20-day-old plants. (B) Top view of the inflorescence meristems of a 20-day-old plant showing expression of VENUS:FD and VENUS:FDP. The samples were cleared and stained with Renaissance. (C) Scatter plot of binned read coverage of the *pFD::VENUS:FD* (lef) and *pFDP::VENUS:FDP* (right) duplicates. Read counts in each 5000-nt bin were normalized to RPKM and then log2-transformed. (D) Overlap size distribution. The histograms show the distribution of the relative overlaps between peak pairs determined as the percentage of the length of the smaller peak that overlaps with the larger peak in FD (left) and FDP (right). The vertical red line shows the cut off used to define overlaps. (E) Venn diagram showing the number of common and unique peaks of the two FD (upper panel) and FDP (lower panel) ChIP-seq replicates. (F) Z-score distribution of number of FD or FDP binding peaks containing multiple instances of a particular hexamer. Vertical red lines indicate the Z-score corresponding to the G-box motif. (G) Density plot for the distance between the consecutive G-box motifs in FD- and FDP- peaks including the promoters (3kb upstream) of all genes except those predicted to be targets of FD or FDP. (H) Box plots corresponding to the signal strength (averaged over replicates) for common, FD-specific and FDP specific peaks. For the common peaks, the signal strengths are given in the FD and FDP data separately. (I) Comparison of FDP and FD binding sites using the endogenous promoters or the *35S* promoter for FDP. Scale bar= 100µm (Aiii, Aiv, B); 50µm (Ai, Aii).

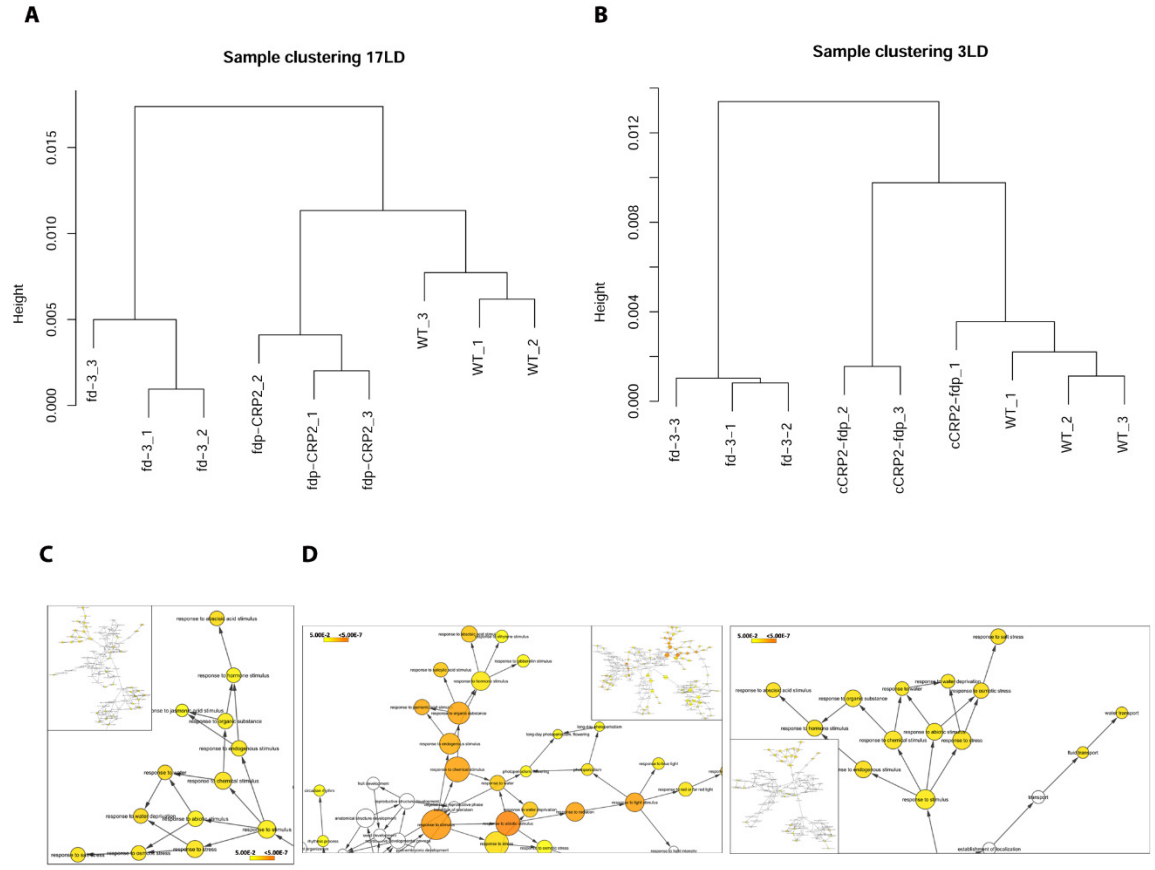

Figure S6. Related to Figure 6. RNA-seqs in *fd* and *fdp* mutants. Complete linkage hierarchical clustering of RNA-seq samples from 17 LDs (A) and 3 DAS (B) using distances derived from pairwise Pearson correlations. (C) GO-term enrichment of the overlapping 19 DEGs in seedlings bound by FD or FDP. (D) GO-term over-representation of the 321 genes differentially expressed and bound by FD (left panel). The inset shows an overview of all GO terms. GO-term enrichment of the 38 genes differentially expressed and bound by FDP (right panel). The colour of the circles reflects the *p*-value and the size represents the over- or under-representation of GO categories according a hypergeometric test (FDR < 0.05). The inset shows an overview of all GO terms. BINGO was used for the GO analysis and Cytoscape for the visualization.

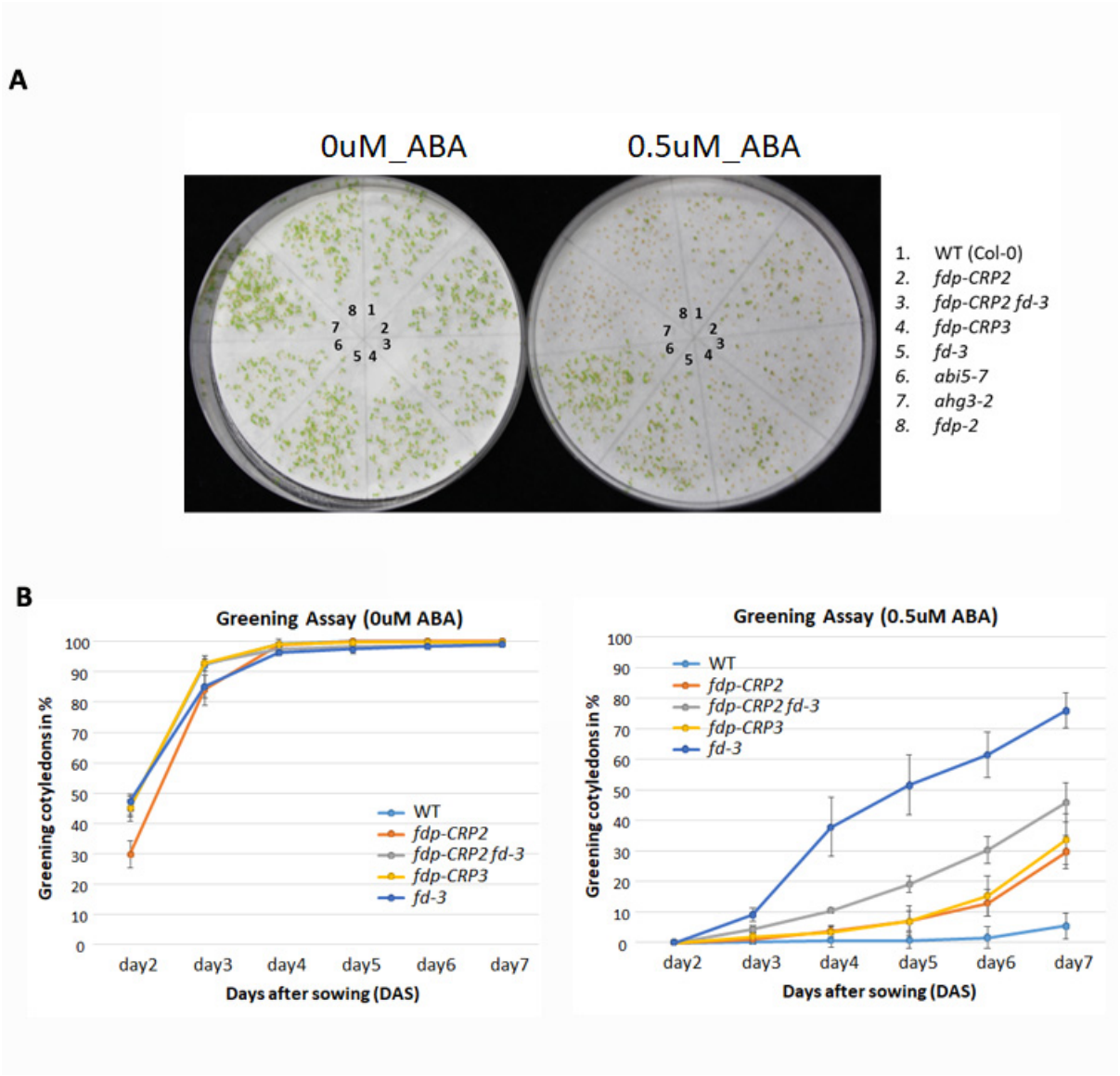

Figure S7. Related to Figure 7. Greening cotyledon analysis on *fdp* and *fd* mutants. (A) Greening cotyledon phenotypes of WT vs. *fd*, *fdp*, *abi5*, *ahg3* single mutants and the *fd fdp* double mutant grown in the absence of ABA (left) or with 0.5 µM ABA (right) for 7 days. (B) Diagram representing the percentage of greening cotyledons (Y-axis) for the illustrated genotypes in the presence of 0.5µM ABA along development, from day 2 to 7. The error bars represent standard errors (SE) of two independent biological replicates.

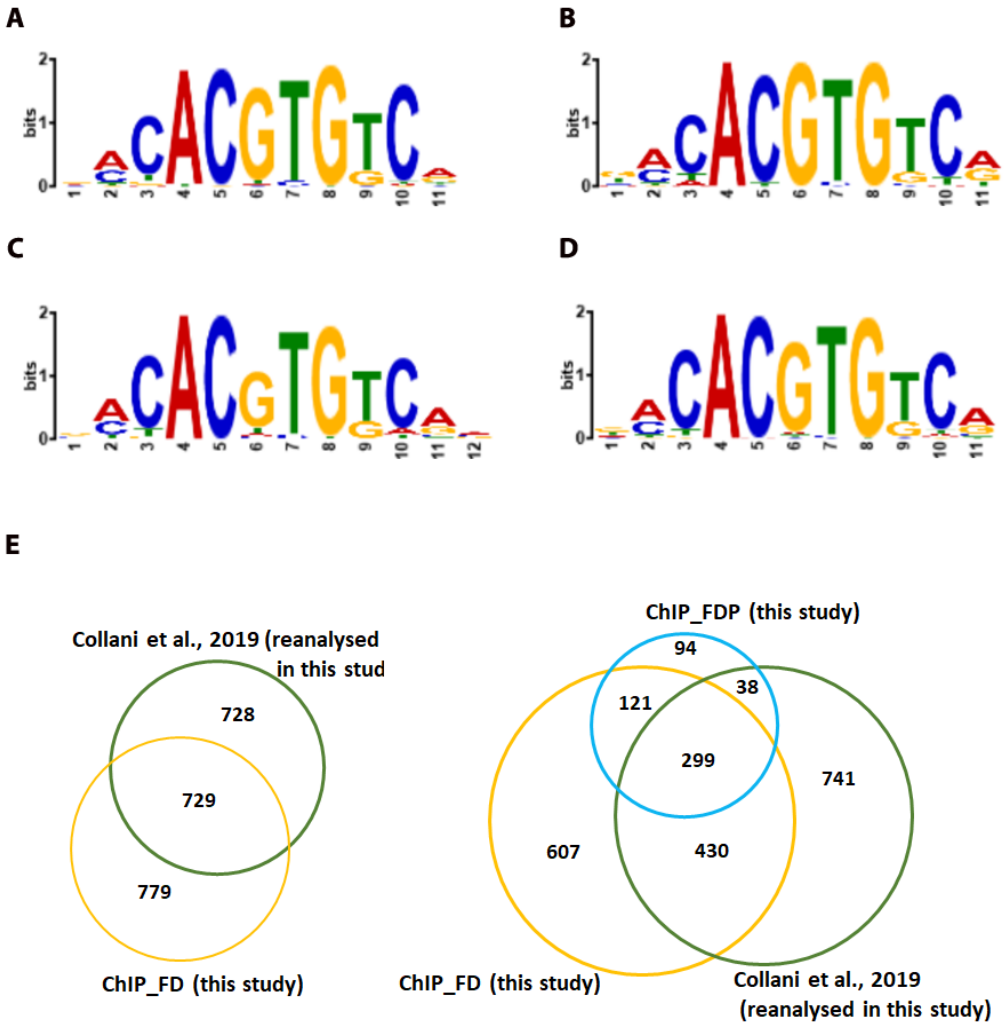

Figure S8. Related to Figure 5. Comparison of FD ChIP-seq data between this study and the previous study of Collani et al (2019). (A) Logo of the enriched sequence motif identified by MEME motif analysis in the whole set of 752 FD peaks (*E*-value = 3.4e-511). (B) Logo of the enriched sequence motif identified by MEME motif analysis in the subset of 109 FD targets bound and differentially expressed in the RNA-seq of 17-LD apices (*E*-value = 1.7e-096). (C) Logo of the enriched sequence motif identified by MEME motif analysis in the subset of

292 FD targets bound and differentially expressed in the RNA-seq of 3-DAS seedlings (*E*-value = 1.6 e-213). (D) Logo of the enriched sequence motif identified by MEME motif analysis in the re-analyzed FD ChIP-seq data from Collani et al., 2019. (*E*-value = 4.5e-652). (E) Venn diagrams showing the overlapping FD targets between the data from Collani et al., 2019 and those in this study (left panel). The raw data from Collani et al. (2019) were reanalyzed it using the same method as for FD and FDP ChIP-seq in this study. In total, 1,457 targets were identified in the new analysis of the data from Collani et al. (2019). The frequency of genes that overlapped between the two data sets was 50% (729 genes out of 1,457), which was statistically significant (*p*-value < 2.2e-16). The overlap between FD and FDP targets from this study and the reanalyzed data-set from Collani et al. (2019) (right panel). In total, 299 (54%) of the total FDP targets were included in the data set from Collani and the current FD data set. (F) Motif Z-score distribution in FD (left) and FDP peaks (right). Vertical lines indicate the Z-scores of the G-box motif (RED) and the additional Collani motif (Green). The white columns show the number of hexamers with a particular Z-score.

Genotypes	**Days to visible floral bud**	**Number of individuals**
Col-0	24.6 ± 1.9[a]	12
fdp-CRP1	22.7 ± 2.0[b]	12
fdp-CRP2	22.1 ± 1.7[b]	12
fdp-CRP3	21.7 ± 1.5[b]	12

Table S1. Related to Figure 1. Days to flower in *fdp* mutants compared to Col-0 and *fd-3*. Flowering time was measured as days to visible floral bud. Two independent biological experiments were performed. Superscript letters indicate the statistical groups to which each genotype belongs (Student's *t* test, $P < 0.05$).